Reaction, diffusion and non-local interaction

H. Ninomiya,[*] Y. Tanaka[†] and H. Yamamoto[‡]

Abstract

Recent years have seen the introduction of non-local interactions in various fields. A typical example of a non-local interaction is where the convolution kernel incorporates short-range activation and long-range inhibition. This paper presents the relationship between non-local interactions and reaction-diffusion systems in the following sense: (a) the relationship between the instability induced by non-local interaction and diffusion-driven instability; (b) the realization of non-local interactions by reaction-diffusion systems. More precisely, it is shown that the non-local interaction of a Mexican-hat kernel destabilizes the stable homogeneous state and that this instability is related to diffusion-driven instability. Furthermore, a reaction-diffusion system that approximates the non-local interaction system with any even convolution kernel is shown to exist.

1 Introduction

Various pattern formations are observed to occur in nature such as those on animal skins, the arrangement of leaves or flowers in plants, and the propagation of the potential in hearts of living creatures and so on. Many researchers have been attracted to these formations over the years and have investigated the mechanisms according to which they are created. In 1952, Turing [20] proposed diffusion-driven instability as one of the mechanisms that is responsible for generating inhomogeneity. He showed that there is a reaction-diffusion system for which the

[*]School of Interdisciplinary Mathematical Sciences, Meiji University, 4-21-1 Nakano, Nakano-ku, Tokyo 164-8525, Japan

[†]Department of Mathematics, Faculty of Science, Hokkaido University, Kita 10, Nishi 8, Kita-ku, Sapporo, Hokkaido, 060-0810, Japan, CREST, Japan Science and Technology Agency

[‡]Organization for the Strategic Coordination of Research and Intellectual Properties, Meiji University, 4-21-1 Nakano, Nakano-ku, Tokyo 164-8525, Japan

homogeneous steady state is unstable, whereas it is stable for the corresponding ordinary differential equations without diffusion. In other words, diffusion can destabilize the homogeneous steady state by being incorporated with kinematics although diffusion is usually thought to function as averaging and homogenizing. This phenomenon is also known as *Turing instability*. We also refer to [2] for the extension to the three-component case. Since the diffusion term is derived from Brownian motion and the reaction term is based on the collision of molecules, we can regard the dynamics of a reaction-diffusion system as *local dynamics* and can also say that it is based on a *local interaction*.

On the other hand, we often observe dynamics that cannot be described in terms of local dynamics. We refer to dynamics of this type as *non-local dynamics* and also consider the corresponding system to be based on a *non-local interaction*. Non-local dynamics have been studied in several fields such as ecology, genetics, neurology, and phase transitions. Typical examples of non-local interactions are spatial dispersals of animal species [11], pigment cells in the skin of the zebrafish [12, 18], and neural firing in the brain [1] etc. See also [6, 8, 16, 17]. These types of interactions can be characterized by convolution with suitable kernels. More precisely, to consider the dynamics of neuron fields in the brain, Amari [1] introduced a neural model in one-dimensional space as follows:

$$\tau\frac{\partial u}{\partial t} = -u + \int_{\mathbb{R}} w(x-y)H(u(y,t))dy + s(x,t), \tag{1}$$

where $u(x,t)$ is the membrane potential of the neurons at position x, $\tau > 0$ is a time constant, w is a kernel, s is an external stimulus, and H is the Heaviside function. The function w represents a non-local effect on the membrane potential from neighboring cells. He realized a short-range activation effect and a long-range inhibitory effect by using the kernel of which the profiles are shown in Fig. 1 (a). The shape of this profile has resulted in this kernel becoming known as the *Mexican-hat*, with reference to [13, 14].

One of the mathematical models for the non-local spatial dispersal of species is as follows:

$$u_t = \int k(x-y)u(y,t)dy - bu + f(u), \tag{2}$$

where $u = u(x,t)$ is the population density of a single species, $k = k(x)$ is a non-negative kernel, b is a positive constant, and f is a nonlinear function of u. Since the kernel k is related to the transition possibility known as the *position jump-process*, the non-negativity of k is often assumed. The derivation of this non-local evolution equation (2) in a bounded domain was reported in [11]. Although the behavior of the dispersal term is similar to that of diffusion, these authors mentioned that the equation of this non-local model was more flexible than the reaction-diffusion equation to describe the dispersal of single species. Additional details are provided in [3, 4, 5, 11, 21]. In the neural firing phenomenon, this equation is also used when the kernel k is replaced with the Mexican-hat kernel w instead of a non-negative kernel [16, 17]. The stationary pattern was investigated numerically [1, 17]. In addition, Kondo pointed out the importance of non-local interaction among pigment cells such as in the skin of the zebra fish and the sensitive dependence of pattern formations on these non-local interactions [12].

Berestycki *et al.* [6] considered the non-local Fisher-KPP equation with the non-local saturation effect:

$$u_t - \Delta u = \mu u \left(1 - k * u\right), \tag{3}$$

where $k(x)$ is a positive kernel and μ is a constant. These non-local competitive effects were introduced by [9, 15]. The classical Fisher-KPP equation corresponds to the case where $k(x) = \delta(x)$.

Non-local evolution equations can reproduce the various patterns and destabilization of the solution is sensitive to the profile of the kernel, such as in the case of the Mexican-hat (see [16, 17]). However, the role of non-local interaction in pattern formations and the mechanism of the appearance of non-local interactions, which can influence distant objects globally without collision in biological phenomena, have not been clarified. This has given rise to questions as to "*What is the relationship between the kernel shape of the non-local evolution equation and the destabilization of the solution?; what is the relationship between non-local interaction and local dynamics such as in a reaction-diffusion system?*". Motivated by these questions, we analyze the mathematical model with non-local interaction. The relationship between the kernel shape and the destabilization of the solution induced by the Mexican-hat is investigated by approximating the non-local evolution equation by the reaction-diffusion system through singular limit analysis. The approximation of the Mexican-hat is shown by introducing the auxiliary activator and inhibitor into the reaction-diffusion system. Moreover, by introducing multiple unknown variables into the system, we show that non-local interaction with any even kernel can be realized by a reaction-diffusion system with multiple components. This result is expected to enable us to conclude that non-local interaction can be reproduced by local dynamics such as those in a chemical reaction and diffusion, which is seemingly paradoxical. Actually, our result can suggest that the non-local interactions in (2) (3) and even (1) can be derived from the reaction-diffusion system. Finally, numerical results are generated by the various shapes of the kernels.

This paper is organized as follows: In Section 2, we state the mathematical setting of the non-local equation considered in this paper and the main result. Section 3 presents the local and global existence of solutions of the non-local equation. In Section 4, we show the instability caused by the non-local effects. Section 5, we construct the reaction-diffusion system that approximates the non-local evolution equation under the assumption of the kernel and study the relationship between two systems from the viewpoint of instability. In Section 6, we show that the reaction-diffusion system constructed in Section 5 approximates the non-local equations with any even kernels by controlling the coefficients. In Section 7, we numerically investigate the profile of the stable stationary solution by varying the shape of the simplified Mexican-hat.

2 Mathematical setting and main result

In this section, we introduce the mathematical setting including non-local interaction. First, we consider a reaction-diffusion equation to represent local dynamics. Denoting the theoretical concentration at the position x at time t by $u(x,t)$, we firstly impose the diffusion and reaction terms as follows:

$$u_t = d_u u_{xx} + f(u), \tag{4}$$

with periodic boundary conditions in $\mathbb{T} := [-L, L]$, where f is a C^1 function from $\mathbb{R}$ to $\mathbb{R}$ and the diffusion coefficient d_u is a non-negative constant. To clarify the questions in Section 1, we extend (4) by adding the non-local interactions including the examples in Section 1. One of the simplest extensions of this reaction-diffusion equation (4) to a non-local evolution equation is

$$(P) \qquad \begin{cases} u_t = d_u u_{xx} + g(u, J * u), & \text{in } \mathbb{T} \times \{t > 0\}, \\ u(x,0) = u_0(x), & \text{on } \mathbb{T}, \end{cases}$$

with the periodic boundary condition in $\mathbb{T}$, where $J \in L^1(\mathbb{T})$ is a kernel, g is a C^1 function from $\mathbb{R}^2$ to $\mathbb{R}$ and $J * h(x) := \int_{-L}^{L} J(x-y)h(y)dy$ for any function $h \in L^1(\mathbb{T})$. A typical example of J is a Gaussian kernel or a Mexican-hat kernel. It is observed in the experiments of [18] that the growth rate of the pigment cells in the skin of the zebra fish is influenced by the neighbours globally in space. Beside the examples in Section 1, the non-local interaction can be included in the growth rate. Thus, for the conditions for f and g, we assume that there are a positive constant g_0 and nonnegative constants $g_1, \cdots, g_7$ and $p \geq 2$ such that, for $u, v \in \mathbb{R}$,

$(A1)$ $\quad f(u) = g(u,0), \quad g(0,0) = g(1,0) = 0,\ g_u(1,0) < 0,\ g_v(1,0) > 0,$

$(A2)$ $\quad g(u,v)u \leq -g_0|u|^{p+1} + g_1|u^2 v| + g_2|uv| + g_3|u|,$

$(A3)$ $\quad \left| g_u(u,v) + g_0 p|u|^{p-1} \right| \leq g_4|v| + g_5,$

$(A4)$ $\quad |g_v(u,v)| \leq g_6|u| + g_7,$

$(A5)$ $\quad p \geq 3$ or $g_1 = g_6 = 0$ if $2 \leq p < 3$.

From $(A1)$ and $(A2)$, we determine the condition of f such that

$$f(u) \leq -g_0|u|^p + g_3$$

for $u \geq 0$, which plays the role of the saturation effect of the concentration. This model can be interpreted by considering that the theoretical living object diffuses and interactions among them are influenced locally as well as globally in space. The condition $(A5)$ can be relaxed to g_1, g_7 are small when $2 \leq p < 3$.

Two typical examples of the local and non-local interaction terms $f(u)$, $g(u,v)$ are

$$f(u) = au(1-u^2), \qquad g(u,v) = uv + au(1-u^2), \tag{5}$$
$$f(u) = au(1-u), \qquad g(u,v) = v + au(1-|u|), \tag{6}$$

where $a > 0$ is a positive parameter. In the case of (5), the non-local interaction is imposed as the growth rate. The corresponding non-local evolution equation becomes

$$\begin{cases} u_t = d_u u_{xx} + (J * u)\,u + f(u), & \text{in } \mathbb{T} \times \{t > 0\}, \\ u(x,0) = u_0(x), & \text{on } \mathbb{T}, \end{cases} \tag{7}$$

where $f(u) = au(1-u^2)$. If J is a Mexican-hat, the growth rate at a point is increased proportionally to the amount of the concentration in close proximity, and conversely, it is decreased proportionally to that of the concentration at greater distances from the point. As the non-local interaction is the convolution, the integration of the global interaction determines whether the concentration at the point is increased or not. We utilize this mathematical model in all the numerical simulations in this paper. The typical example of J is given by

$$J(x) := \frac{\mu}{2\sqrt{d_1}\sinh\frac{L}{\sqrt{d_1}}}\cosh\frac{L-|x|}{\sqrt{d_1}} - \frac{\mu}{2\sqrt{d_2}\sinh\frac{L}{\sqrt{d_2}}}\cosh\frac{L-|x|}{\sqrt{d_2}}, \tag{8}$$

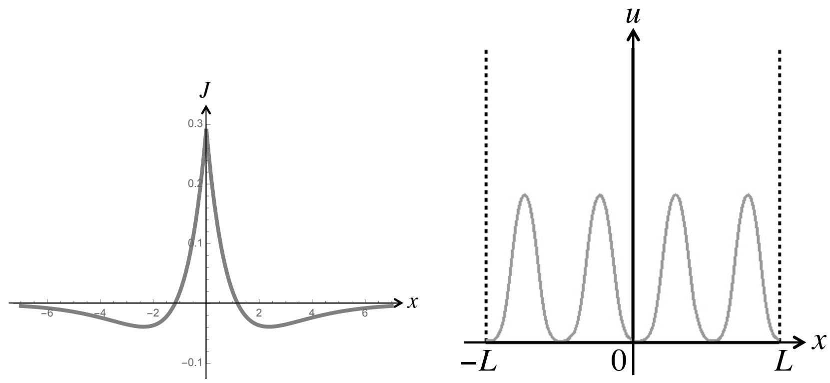

(a) Profile of the kernel J (b) Numerics of (P)

Figure 1: (a) Typical example of the kernel (8), at which $d_1 = 1$, $d_2 = 2$, $\mu = 1$ and $L = 20$. The vertical and horizontal axes correspond to the value of $J(x)$ and the position $x \in [-L, L]$, respectively. The profile of this kernel is similar to the shape of the Mexican-hat because of the short-range activation near the origin and long-range inhibition at greater distances. (b) Numerics of (7) with $d_u = 0.1$, $a = 0.02$, and the same kernel $J(x)$ as in (a). The vertical and horizontal axes correspond to the value of u and the position $x \in \mathbb{T}$, respectively

.

where d_1, d_2 and μ are positive constants. Fig. 1 (a) is the profile of J when $\mu = 1, d_1 = 1, d_2 = 2$. As seen in Fig. 1 (b), (7) creates the heterogeneity solutions with 4 peaks.

In the case of (6), the non-local interaction is imposed as dispersal and thus, J should be non-negative from the viewpoint of mathematical modelling. However, the following results can include the case of the sign-changing kernel J.

It is easily verified that two examples (5) and (6) satisfy $(A1)$–$(A5)$. The example (2) is directly included in (P) and satisfies $(A1)$–$(A5)$. For (1) and (3), see Remark 6.2 in Section 6.

Under the above settings, the main result in this paper is as follows:

Theorem 2.1 (Main theorem) *For any even $2L$-periodic continuous function J, any small positive constant ε and any positive time T, there exists a reaction-diffusion system (RD^{ε}) with $M+2$ components such that*

$$\sup_{t\in[0,T]} \sup_{-L\le x\le L} |u(x,t) - \widetilde{u}(x,t)| \le \varepsilon,$$

where (RD^{ε}) is given in Section 6, u is a solution of (P), and $\widetilde{u}$ is the first component of the solution of (RD^{ε}).

The proof of this theorem, which is given in Section 6, needs to find out the values of constants M, α_j and d_j $(j = 0, \cdots, M)$ in (RD^{ε}). See Section 6 for the details.

3 Existence of the solution in (P)

In this section we study the global existence of the solution of (P). Before introducing our results, we give some definitions as follows:

$$
\begin{aligned}
&C_{per}(\mathbb{T}) = \{u \in C(\mathbb{R}) \mid u(x) = u(x+2L)\},\\
&\|v\|_{C_{per}(\mathbb{T})} = \sup_{x\in\mathbb{T}} |v(x)| \quad \text{for any} \quad v \in C_{per}(\mathbb{T}),\\
&A := -\frac{\partial^2}{\partial x^2} \quad \text{with} \quad D(A) := C^2_{per}(\mathbb{T}),\\
&B(u,r) := \{v \in C_{per}(\mathbb{T}) \mid \|u-v\|_{C_{per}(\mathbb{T})} \le r\}.
\end{aligned}
$$

Theorem 3.1 *For each $u_0 \in C_{per}(\mathbb{T})$, there exists a positive constant T such that the problem (P) has a unique mild solution $u(\cdot;u_0) \in C([0,T];C_{per}(\mathbb{T}))$ with an initial datum u_0 which satisfies*

$$u(t) = e^{-d_u tA}u_0 + \int_0^t e^{-d_u(t-s)A} g(u(s), J*u(s))\,ds.$$

Moreover, there exists a positive constant K_1 such that for $u_0, u_1 \in B(\bar{u}, r)$ mild solutions $u(\cdot;u_0)$ and $u(\cdot;u_1)$ of (P) with initial data u_0 and u_1, respectively satisfy the following

$$\|u(t;u_0) - u(t;u_1)\|_{C_{per}(\mathbb{T})} \le K_1 \|u_0 - u_1\|_{C_{per}(\mathbb{T})}.$$

This theorem follows from the standard semigroup theory [10, Theorem 1.3.4]. Denote a solution of (P) by $u(x,t) = u(x,t;u_0)$. We note that $u(x,t;u_0) = u(t;u_0)(x)$ because of $u(\cdot;u_0) \in C_{per}(\mathbb{T})$. Furthermore, by the energy method we obtain the following theorem:

Theorem 3.2 *Assume that $u(\cdot,0) = u_0(\cdot) \in H^1(\mathbb{T})$ and $d_u > 0$. Then, there exists a positive constant K_2 depending on $\|u_0\|^2_{H^1(\mathbb{T})}$ such that, for all $t > 0$, the mild solution u of (P) with the initial datum u_0 satisfies*

$$\|u(\cdot,t)\|^2_{H^1(\mathbb{T})} \le K_2.$$

The proof is given in Appendix A.2.

Remark 3.1 *From this theorem and the Sobolev embedding theorem, we see that* $\|u(\cdot,t)\|_{C_{per}(\mathbb{T})}$ *is bounded for* $t > 0$*. Hence, we have the global existence of the classical solution of* (*P*)*. However, our proof in Appendix A.2 can not be extended to the case of* $d_u = 0$ *because* K_2 *depends on* $1/d_u$ *.*

4 Instability induced by non-local terms

Assume that

$$(A6) \qquad \int_{\mathbb{T}} J(x)dx = 0.$$

When a solution of (P) is spatially homogeneous, it satisfies

$$U_t = g(U,0). \tag{9}$$

In other words, any solution of (9) becomes a spatially homogeneous solution of (P). Under the assumption $(A1)$, $U^* \equiv 1$ is a stable equilibrium of (9) and is a constant steady-state solution of (P). To study the stability, we consider the linearized problem of (P) at $U^* \equiv 1$. Noting $J * 1 = 0$ by $(A6)$, we have

$$\lambda\varphi = d_u\varphi_{xx} + g_u(1,0)\varphi + g_v(1,0)J * \varphi. \tag{10}$$

Here we used $(A6)$. Plugging the kth term of the Fourier series expansion

$$\varphi_k := c_k \exp\left(\frac{k\pi i}{L}x\right), \quad c_k := \frac{1}{2L}\int_{-L}^{L} \varphi(x)\exp\left(-\frac{k\pi i}{L}x\right)dx$$

to (10), we obtain

$$\lambda\varphi_k = -d_u\left(\frac{k\pi}{L}\right)^2\varphi_k + g_u(1,0)\varphi_k + g_v(1,0)J * \varphi_k.$$

Since J is a periodic function in $\mathbb{T}$, it follows

$$J * \varphi_k = 2L(\widehat{J})_k\varphi_k,$$

where

$$(\widehat{J})_k := \frac{1}{2L}\int_{-L}^{L} J(y)\exp\left(-\frac{k\pi i}{L}y\right)dy.$$

Thus all eigenvalues are given by

$$\lambda = -d_u \left(\frac{k\pi}{L}\right)^2 + g_u(1,0) + 2L(\widehat{J})_k g_v(1,0). \tag{11}$$

Thus we obtain the following proposition:

Proposition 4.1 *Assume that $g(u,v)$ enjoys $(A1)$ and $J(x) = \mu j(x)$ does the following condition:*

$$(A7) \qquad (\widehat{J})_k = \mu(\widehat{j})_k > 0 \quad (k > 0), \quad (\widehat{j})_0 = 0, \quad \lim_{k\to\infty}(\widehat{j})_k = 0.$$

Then there is a positive constant μ^* such that $U^* \equiv 1$ is stable in (P) if $0 \leq \mu < \mu^*$, but is unstable in (P) if $\mu > \mu^*$.

We remark that the condition $(\widehat{j})_0 = 0$ corresponds to $(A6)$. This proposition is essentially mentioned in Murray [17, Chap 12].

Proof. By (11) and $(A7)$, if $\lambda = 0$, then it follows

$$\mu = \mu(k) := \frac{d_u\left(\frac{k\pi}{L}\right)^2 - g_u(1,0)}{2L(\widehat{j})_k g_v(1,0)}.$$

Since $\mu(k)$ diverges to infinity as k tends to infinity by $(A1)$ and $(A7)$, there is a positive integer k^* such that

$$\mu(k^*) = \min_k \mu(k).$$

Then the eigenvalue λ is still negative for all k if $0 \leq \mu < \mu(k^*)$, while λ becomes positive for the minimizer k^* of μ if $\mu(k^*) < \mu$. Hence, we have the proposition. □

As for the typical example given in (8), we can calculate

$$(\widehat{J})_k = \frac{\mu}{d_1\left(\frac{k\pi}{L}\right)^2 + 1} - \frac{\mu}{d_2\left(\frac{k\pi}{L}\right)^2 + 1}.$$

It is easily seen that this function J satisfies $(A7)$ and that the stationary solution U^* becomes unstable if μ is large. More precisely, the most unstable mode can be determined by the following calculation. The eigenvalue λ is therefore given by

$$\lambda(\sigma_k) = -d_u\sigma_k + \left(\frac{\mu}{d_1\sigma_k+1} - \frac{\mu}{d_2\sigma_k+1}\right) g_v(1,0) + g_u(1,0), \qquad (12)$$

where $\sigma_k := (k\pi/L)^2$, $k \in \mathbb{N}\cup\{0\}$. We determine that this λ has at least a positive value dependently of the value of σ_k. Setting the sufficiently large L, we regard σ_k as the continuous value. Rewriting $\sigma_k = s$, we have

$$\lambda(s) = \left(\frac{-d_u d_1 d_2 s^3 - d_u(d_1+d_2)s^2 + (-d_u + (d_2-d_1)\mu g_v(1,0))s}{(d_1 s+1)(d_2 s+1)}\right)\Big|_{s=\sigma_k} + g_u(1,0)$$

for $s \geq 0$. When $d_2 > d_1$, if

$$\mu > \frac{d_u}{g_v(1,0)(d_2-d_1)},$$

then $\lambda(s)$ attains a positive maximum at $s = s_c > 0$. Moreover, if $d_u = 0$, it follows from the easy calculation that the maximum eigenvalue is attained by the wave number $k^* := L(d_1d_2)^{-1/4}/\pi$. When $g(u,v)$ is given by (5), $\lambda(\sigma_k)$ is numerically calculated as seen in Fig. 2 (a). From this figure, the maximum eigenvalue is attained by $k = 4$ and this wave number corresponds to the number of peaks shown in Fig. 1 (b).

5 Convergence of the reaction-diffusion system to a non-local evolution equation

5.1 The reaction-diffusion system and its convergence

In this section let us consider the case where J is the linear combination of the functions, i.e.,

$$J = \mu \sum_{j=0}^{M} \alpha_j k^{d_j}, \qquad (13)$$

where $d_j > 0$, α_j are constants and

$$k^d(x) := \frac{1}{2\sqrt{d}\sinh\frac{L}{\sqrt{d}}} \cosh\frac{L-|x|}{\sqrt{d}}. \qquad (14)$$

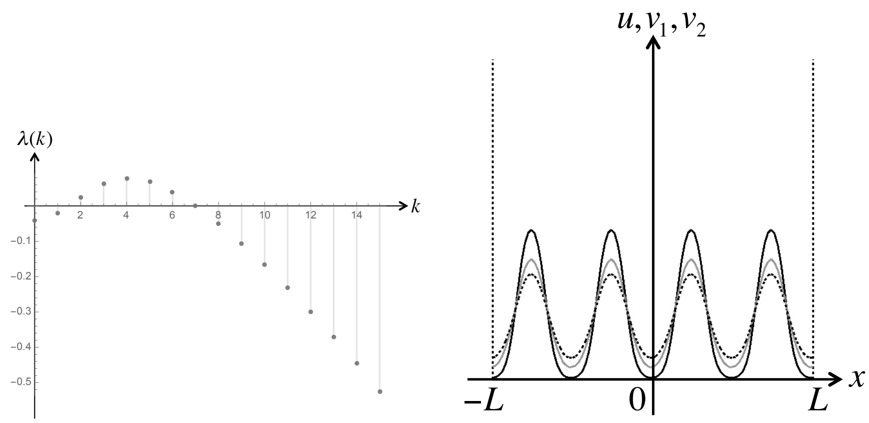

(a) Graph of $\lambda(\sigma_k)$ (b) Profiles of u, v_1 and v_2

Figure 2: Numerical results of the system (15) with the same function $g(u,v) = uv + au(1-u^2)$ and parameters as in Fig. 1 (b) and $\varepsilon = 0.001$. (a) Relationship between k and $\lambda(\sigma_k)$. The vertical and horizontal axes correspond to the value of $\lambda(\sigma_k)$ and the wave number k, respectively. From this graph, $\lambda(\sigma_k)$ attains its maximum when $k = 4$. (b) Profiles of u, v_1 and v_2 of the system (15). The vertical and horizontal axes correspond to the values of u, v_1, v_2 and the position $x \in \mathbb{T}$, respectively. The black solid, gray solid and dashed curves correspond to the profiles of u, v_1 and v_2, respectively.

We introduce a reaction-diffusion system with auxiliary activators and inhibitors $v_j(x,t), (j = 0, \cdots, M)$ that approximates a non-local evolution equation (P) with (13):

$$(RD^{\varepsilon}) \qquad \begin{cases} u_t &= d_u u_{xx} + g(u, \sum_{j=0}^{M} \alpha_j v_j), \\ v_{j,t} &= \dfrac{1}{\varepsilon}\left(d_j v_{j,xx} + \mu u - v_j\right) \end{cases}$$

for $x \in \mathbb{T}$ and $t > 0$ with the periodic boundary condition, where all diffusion coefficients d_j and μ are positive, and $0 < \varepsilon \ll 1$. Taking limit $\varepsilon \to 0$ formally in (RD^{ε}), we may expect that v_j converge to a stationary solution respectively. Namely,

$$d_j v_{j,xx} + \mu u - v_j = 0.$$

As in Appendix A.1, v_j is given by

$$v_j = \mu k^{d_j} * u.$$

Because μ is a fixed value, we set $\mu = 1$ for the simplicity in the following singular limit analysis. This convergence will be rigorously confirmed as follows.

Theorem 5.1 *Assume that J is given by* (13)*. Let u^0 be a solution of* (P) *equipped with $u(\cdot,0) = u_0(\cdot) \in H^1(\mathbb{T})$ and $(u^\varepsilon, v_0^\varepsilon, \cdots, v_M^\varepsilon)$ be a solution of* (RD^ε) *equipped with*

$$(u^\varepsilon, v_0^\varepsilon, \cdots, v_M^\varepsilon)(x,0) = (u_0, k^{d_0} * u_0, \cdots, k^{d_M} * u_0).$$

Then, for any positive T,

$$\sup_{t\in[0,T]} \|u^\varepsilon(\cdot,t) - u^0(\cdot,t)\|_{C_{per}(\mathbb{T})} \to 0,$$
$$\sup_{t\in[0,T]} \|v_j^\varepsilon(\cdot,t) - k^{d_j} * u^0(\cdot,t)\|_{C_{per}(\mathbb{T})} \to 0 \qquad (j = 0, \cdots, M)$$

as $\varepsilon \to 0$.

The proof will be given in Appendix B. It is based on the standard arguments, such as the energy method, the uniform Gronwall lemma, the positively invariant set. The proof of boundedness of solutions in $H^1(\mathbb{T})$ is similar to that of Theorem 3.2. See Lemma B.1 in Appendix B. Using this lemma and the energy estimate for the difference between two solutions, we can show the convergence. See Appendix B for the details.

5.2 Diffusion-driven instability

Consider the Mexican hat kernel (8). Since this satisfies ($A6$), we use v_1 and v_2 instead of v_0 and v_1. The corresponding reaction-diffusion system (RD^ε) with $0 < d_1 < d_2$ and $\alpha_1 = 1,\ \alpha_2 = -1$ becomes

$$\begin{cases} u_t &= d_u u_{xx} + g(u, v_1 - v_2), \\ v_{1,t} &= \dfrac{1}{\varepsilon}\left(d_1 v_{1,xx} + \mu u - v_1\right), \\ v_{2,t} &= \dfrac{1}{\varepsilon}\left(d_2 v_{2,xx} + \mu u - v_2\right). \end{cases} \tag{15}$$

Theorem 5.1 claims that $J * u$ is approximated by $v_1 - v_2$, where J is given in (8) and that the solution of (15) is sufficiently close to that of (P). In the other words, this indicates that the non-local interaction with the kernel (13) can be approximated by the reaction-diffusion system.

By $(A1)$, this reaction-diffusion system consists of two activators and one inhibitor. It is well known that diffusion-driven instability is often observed in this type of reaction-diffusion systems [20]. As shown in the Section 4, the stable homogeneous stationary solution may become unstable by the non-local interaction under suitable assumptions. We discuss the relationship between two instabilities in this subsection.

Anma and Sakamoto [2] studied diffusion-driven instability for the three-component reaction-diffusion system and classified the instability into two categories, one is the instability without oscillation, called *steady instability*, and the other is the instability with oscillations, called *wave instability*. By Theorem 1.1 (v) of [2], the system (15) satisfies the condition of the occurrence of the steady instability in the steady state. We show the instability of the homogeneous stationary solution $(u,v_1,v_2)=(1,\mu,\mu)$ to (15) when ε is close to 0. Linearizing (15) near $(u,v_1,v_2)=(1,\mu,\mu)$, we obtain the following eigenvalue problem:

$$\lambda\begin{pmatrix} u \\ v_1 \\ v_2 \end{pmatrix}=\begin{pmatrix} -d_u\sigma_k+g_u(1,0) & g_v(1,0) & -g_v(1,0) \\ \frac{\mu}{\varepsilon} & \frac{-1-d_1\sigma_k}{\varepsilon} & 0 \\ \frac{\mu}{\varepsilon} & 0 & \frac{-1-d_2\sigma_k}{\varepsilon} \end{pmatrix}\begin{pmatrix} u \\ v_1 \\ v_2 \end{pmatrix},$$

where $\sigma_k := (k\pi/L)^2,\ k\in\mathbb{N}\cup\{0\}$ and λ is the eigenvalue of linearized matrix. We denote the characteristic polynomial by $\Phi_k(\varepsilon,\lambda)$. We get

$$\begin{aligned}\Phi_k(\varepsilon,\lambda) \;=\;& \frac{1}{\varepsilon^2}\left(\mu g_v(1,0)(d_2-d_1)\sigma_k-(d_u\sigma_k-g_u(1,0)+\lambda)(1+d_1\sigma_k)(1+d_2\sigma_k)\right) \\ &-\frac{\lambda}{\varepsilon}(d_u\sigma_k-g_u(1,0)+\lambda)(2+d_1\sigma_k+d_2\sigma_k) \\ &-\lambda^2(d_u\sigma_k-g_u(1,0)+\lambda).\end{aligned} \tag{16}$$

Set

$$\widetilde{\Phi}_k(\varepsilon,\lambda):=\varepsilon^2\Phi_k(\varepsilon,\lambda).$$

Solving $\widetilde{\Phi}_k(0,\lambda)=0$, we have

$$\begin{aligned}\lambda =&\frac{\mu g_v(1,0)(d_2-d_1)\sigma_k-(d_u\sigma_k-g_u(1,0))(1+d_1\sigma_k)(1+d_2\sigma_k)}{(1+d_1\sigma_k)(1+d_2\sigma_k)} \\ =&-d_u\sigma_k+\left(\frac{\mu g_v(1,0)}{1+d_1\sigma_k}-\frac{\mu g_v(1,0)}{1+d_2\sigma_k}\right)+g_u(1,0).\end{aligned}$$

We remark that this eigenvalue corresponds to (11). We denote it by $\lambda^0(k)$. Moreover, we see that

$$\frac{\partial}{\partial\lambda}\widetilde{\Phi}_k(0,\lambda) = -(1+d_1\sigma_k)(1+d_2\sigma_k) < 0,$$

for arbitrary $k \in \mathbb{N}\cup\{0\}$ and $\lambda \in \mathbb{R}$. The implicit function theorem guarantees that, for small ε, there exists the unique root $\lambda^\varepsilon(k)$ of $\widetilde{\Phi}_k(\varepsilon,\lambda) = 0$ and $\lim_{\varepsilon\to 0}\lambda^\varepsilon(k) = \lambda^0(k)$.

Next, (16) can be rewritten in the descending order of λ as

$$\begin{aligned}
\Phi_k(\varepsilon,\lambda) = &-\lambda^3 - \frac{\lambda^2}{\varepsilon}\{(2+d_1\sigma_k+d_2\sigma_k)+\varepsilon(d_u\sigma_k - g_u(1,0))\}\\
&-\frac{\lambda}{\varepsilon^2}\{(1+d_1\sigma_k)(1+d_2\sigma_k)+\varepsilon((d_u\sigma_k-g_u(1,0))(2+d_1\sigma_k+d_2\sigma_k))\}\\
&-\frac{1}{\varepsilon^2}\{\mu g_v(1,0)(d_1-d_2)\sigma_k+(d_u\sigma_k-g_u(1,0))(1+d_1\sigma_k)(1+d_2\sigma_k)\}\\
=&-\lambda^3-\frac{C_1+\varepsilon C_2}{\varepsilon}\lambda^2-\frac{C_3+\varepsilon C_4}{\varepsilon^2}\lambda-\frac{C_5}{\varepsilon^2},
\end{aligned}$$

where $C_1,\cdots,C_5$ are the corresponding real coefficients independently of ε. We note that $C_1 = 2+d_1\sigma_k+d_2\sigma_k > 0$ and $C_3 = (1+d_1\sigma_k)(1+d_2\sigma_k) > 0$. We denote three eigenvalues λ by $\alpha^\varepsilon(k), \beta^\varepsilon(k)$ and $\gamma^\varepsilon(k)$. Since we have already known that one of roots of $\Phi_k(\varepsilon,\lambda) = 0$ is $\lambda^\varepsilon(k)$, we take $\gamma^\varepsilon(k) = \lambda^\varepsilon(k)$. From the Vieta's formulas, we obtain that

$$\alpha^\varepsilon+\beta^\varepsilon+\gamma^\varepsilon = -\frac{C_1+\varepsilon C_2}{\varepsilon}, \quad \alpha^\varepsilon\beta^\varepsilon+\beta^\varepsilon\gamma^\varepsilon+\gamma^\varepsilon\alpha^\varepsilon = \frac{C_3+\varepsilon C_4}{\varepsilon^2}.$$

Because γ^ε converges to γ^0, $|\gamma^\varepsilon|$ is bounded for small ε. Thus, solving the above simultaneous equations of α^ε and β^ε, we see that

$$\alpha^\varepsilon = \frac{-C_1+\sqrt{C_1^2-4C_3}}{2\varepsilon}+\mathscr{O}(1), \quad \beta^\varepsilon = \frac{-C_1-\sqrt{C_1^2-4C_3}}{2\varepsilon}+\mathscr{O}(1).$$

By the fact that C_1 and C_3 are positive, $\mathrm{Re}\,\alpha^\varepsilon, \mathrm{Re}\,\beta^\varepsilon \to -\infty$ as $\varepsilon \to 0$. This implies that there exists no eigenvalues with positive real part except for $\gamma^\varepsilon(k)$ with $\varepsilon \to +0$. Recall that the eigenvalue $\gamma^0(k)$ is equal to $\lambda(\sigma_k)$ given in (11). It turns out that when the equilibrium solution $u = 1$ of (P) becomes unstable, the corresponding eigenvalue γ^ε becomes positive. Therefore the non-local interaction induced instability of (P) can be regarded as diffusion-driven instability of (RD^ε).

Fig. 2 (a) shows the eigenvalue $\gamma^0(k)$. From this diagram, it is obvious that the stationary solution $u=1$ of (P) is unstable and that the stationary solution $(1,1,1)$ of (RD^ε) is also unstable. Furthermore, Fig. 2 (b) shows an inhomogeneous stationary solution of (RD^ε) with four peaks which bifurcates from $(1,1,1)$.

6 Realization of non-local interactions

In Section 5.2, we studied the case where $J=\mu\sum\alpha_j k^{d_j}$. In this section we consider the realization of a non-local evolution equation with a general function J by a reaction-diffusion system (RD^ε) with $M+2$ components. For simplicity, we take $\mu=1$ in this section. Then we consider the system

$$(RD^\varepsilon) \qquad \begin{cases} u_t &= d_u u_{xx} + g(u, \displaystyle\sum_{j=0}^{M} \alpha_j v_j), \\ v_{j,t} &= \dfrac{1}{\varepsilon}\left(d_j v_{j,xx} + u - v_j\right), \end{cases}$$

with the periodic boundary condition. As seen in Section 5.2, this system for (u,v_1,v_2) reproduces the Mexican-hat interaction (8). In this section we consider the question: *what kinds of the kernel J can be approximated by reaction-diffusion systems ?* By Theorem 5.1, the non-local evolution with a kernel $J=\sum_{j=0}^{M}\alpha_j k^{d_j}$ can be approximated by the reaction-diffusion system (RD^ε). Therefore our question is rewritten as "*what kinds of J can be approximated by the finite linear sum of* $\cosh[(L-|x|)/\sqrt{d_j}]$ *?*". Set $d_j=1/j^2$ for $j=1,\cdots,M$ and d_0 will be determined later. Because $\{\cosh j(L-|x|)\}_{j=0}^{M}$ are even functions, so is the linear sum. Therefore we only consider a function $J(x)$ in $[0,L]$. Thus we show the following theorem.

Theorem 6.1 *Every $\phi\in C([0,L])$ is uniformly approximated by a finite linear combination of a family $\{\cosh j(L-x)\}_{j=0}^{\infty}$ of hyperbolic cosines.*

Proof. We take an arbitrary $\phi\in C([0,L])$. Set $y:=\cosh(L-x)$. It is easily seen that y belongs to the interval $I:=[1,\cosh L]$. Then, using the one-to-one correspondence $x=L-\log(y+\sqrt{y^2-1})$, we define a continuous function $\psi(y):=\phi(L-\log(y+\sqrt{y^2-1}))$ on I. By the Stone-Weierstrass theorem, we can approximate $\psi(y)$ by a polynomial function. Actually, for $\varepsilon>0$ there exists a polynomial function $p(y)=\sum_{j=0}^{m}\beta_j y^j$ such that

$$|\psi(y)-p(y)|<\varepsilon$$

for all $y \in I$. Since we put $y = \cosh(L-x)$ and $\psi(y) = \phi(x)$, it follows that

$$|\phi(x) - p(\cosh(L-x))| < \varepsilon \tag{17}$$

for all $x \in [0, L]$. Next, we show that $p(\cosh(L-x))$ is expressed by a finite linear combination of the functions $\cosh k(L-x)$ for $k \in \mathbb{N} \cup \{0\}$. Firstly, we represent y^j for $j \in \mathbb{N} \cup \{0\}$ by a finite linear combination of $\{\cosh k(L-x)\}_{k=0}^{j}$. From

$$2\cosh\alpha \cdot \cosh\beta = \cosh(\alpha+\beta) + \cosh(\alpha-\beta),$$

we see that

$$y^0 = \cosh 0, \quad y^1 = \cosh(L-x), \quad y^2 = \cosh^2(L-x) = \frac{1}{2}\cosh 2(L-x) + \frac{1}{2}.$$

To use the inductive method, we assume that y^j is expressed by a finite linear combination of $\cosh k(L-x)$ for $0 \le k \le j$, that is,

$$y^j = \sum_{k=0}^{j} a_k^{(j)} \cosh k(L-x),$$

where $a_k \in \mathbb{R}$. Calculating y^{j+1} by using this assumption, we have

$$\begin{aligned} y^{j+1} &= \cosh(L-x) \sum_{k=0}^{j} a_k^{(j)} \cosh k(L-x) \\ &= \sum_{k=0}^{j} \frac{a_k^{(j)}}{2} \{\cosh(k+1)(L-x) + \cosh(k-1)(L-x)\} \\ &= \sum_{k=0}^{j+1} a_k^{(j+1)} \cosh k(L-x), \end{aligned}$$

where

$$a_k^{(j+1)} = \begin{cases} \dfrac{a_1^{(j)}}{2} & (k=0), \\ a_0^{(j)} + \dfrac{a_2^{(j)}}{2} & (k=1), \\ \dfrac{a_{k-1}^{(j)} + a_{k+1}^{(j)}}{2} & (2 \le k \le j), \\ \dfrac{a_j^{(j)}}{2} & (k = j+1). \end{cases}$$

Hence, we can express y^{j+1} by a finite linear combination of $\cosh k(L-x)$ for $0 \le k \le j+1$.

Recalling that $p(y) = \sum_{j=0}^{m} \beta_j y^j$, we have

$$p(\cosh(L-x)) \ = \ p(y) = \sum_{j=0}^{m} \beta_j y^j = \sum_{j=0}^{m}\sum_{k=0}^{j} \beta_j a_k^{(j)} \cosh k(L-x) = \sum_{k=0}^{m} \widetilde{\alpha}_k \cosh k(L-x),$$

where $\widetilde{\alpha}_k = \sum_{j=k}^{m} \beta_j a_k^{(j)}$. Since $p(\cosh(L-x))$ is a finite linear combination of $\{\cosh k(L-x) \mid k \in \mathbb{N} \cup \{0\}\}$ and (17) holds for all $x \in [0,L]$, eventually we see that $p(\cosh(L-x))$ is just an uniformly approximation of the continuous function $\phi(x)$. □

Thus by determining d_0, we have the following corollary.

Corollary 6.1 *For any even continuous function $J \in C_{per}(\mathbb{T})$ and any small positive constant ε, there exist a natural number M and constants $d_0, \cdots, d_M, \alpha_0, \cdots, \alpha_M$ such that*

$$\Big\| \sum_{j=0}^{M} \alpha_j k^{d_j} - J \Big\|_{C_{per}(\mathbb{T})} \le 2\varepsilon. \tag{18}$$

We note that $v_j := k^{d_j} * u$ $(j = 0, \cdots, M)$ satisfies

$$d_j v_{j,xx} + u - v_j = 0$$

and enjoys periodic boundary conditions. Then,

$$\Big\| \sum_{j=0}^{M} \alpha_j v_j - J * u \Big\|_{C_{per}(\mathbb{T})} \le 2\varepsilon \|u\|_{L^1(\mathbb{T})}$$

for any function $u(\cdot,t) \in L^1(\mathbb{T})$.

Proof. By Theorem 6.1, for any $\varepsilon > 0$, there are a natural number M and a series of constants $\{\widetilde{\alpha}_j\}_{j=0}^{M}$ such that

$$\Big| J(x) - \sum_{j=0}^{M} \widetilde{\alpha}_j \cosh j(L-|x|) \Big| \le \varepsilon$$

for any $x \in \mathbb{T}$. Set

$$d_j = \frac{1}{j^2}, \quad \alpha_j := \frac{2\widetilde{\alpha}_j}{j} \sinh jL, \qquad (j = 1, \cdots, M).$$

In the case of $j=0$, choose a positive constant d_0 so large as to

$$\left\| \frac{\widetilde{\alpha}_0}{2\sqrt{d_0}\sinh\frac{L}{\sqrt{d_0}}}\cosh\frac{L-|\cdot|}{\sqrt{d_0}} - \widetilde{\alpha}_0 \right\|_{C_{per}(\mathbb{T})} \leq \varepsilon$$

and we set $\alpha_0 = \widetilde{\alpha}_0$. Then

$$\left\| \sum_{j=0}^{M} \frac{\alpha_j}{2\sqrt{d_j}\sinh\frac{L}{\sqrt{d_j}}}\cosh\frac{L-|\cdot|}{\sqrt{d_j}} - J(\cdot) \right\|_{C_{per}(\mathbb{T})} \leq 2\varepsilon.$$

This immediately implies (18). The proof of this corollary has been completed. □

Lemma 6.1 *Suppose that $J_1, J_2 \in C_{per}(\mathbb{T})$ and let u_j $(j=1,2)$ denote the solution of*

$$\begin{cases} u_{j,t} = d_u u_{j,xx} + g(u_j, J_j * u_j), & \text{in } \mathbb{T}\times\{t>0\}, \\ u_j(x,0) = u_0(x), & \text{on } \mathbb{T} \end{cases}$$

respectively. Then for any positive T, there exists a positive constant C_T such that

$$\sup_{t\in[0,T]} \|u_1 - u_2\|_{C_{per}(\mathbb{T})} \leq C_T \|J_1 - J_2\|_{L^1(\mathbb{T})}.$$

We will give a proof of this lemma in Appendix B.2.

Proof of Theorem 2.1. Theorem 2.1 immediately follows from Corollary 6.1 and Lemma 6.1. □

Remark 6.1 *This corollary tells us that any even convolution kernel can be realized by increasing the number of components of reaction-diffusion system. In other words, if many chemical substances are involved, various non-local interactions with even kernels can be realized. Moreover, coefficients of linear combinations are important to specify non-local interactions.*

Remark 6.2 *Since the function u is arbitrary at the equation of v_j in this theorem, by replacing u with the Heaviside function $H(u)$, the model (1) for the neural firing phenomenon by Amari [1] is also approximated by a reaction-diffusion system:*

$$\begin{cases} u_t = d_u u_{xx} + \displaystyle\sum_{j=0}^{M} \alpha_j v_j - u + s(x,t), \\ d_j v_{j,xx} + H(u) - v_j = 0, \qquad (j=0,\cdots,M). \end{cases}$$

For the case of (3)*, Theorem 2.1 is not directly applicable because the assumptions of g are not satisfied. Since the maximum principle implies the non-negativity of solutions of u of* (3) *and* u^{ε} *of* (RD^{ε})*, we can obtain the boundedness of solutions of* (3) *and* (RD^{ε}) *for a finite time.*

One may expect that this corollary can be extended to the non-local evolution equation

$$\begin{cases} u_t = d_u u_{xx} + g(u, J_1 * u, J_2 * u, \cdots, J_K * u), & \text{in } \mathbb{T} \times \{t > 0\}, \\ u(x,0) = u_0(x), & \text{on } \mathbb{T}, \end{cases}$$

where even kernels $J_k \in C_{per}(\mathbb{T})$ $(j = 1, \cdots, K)$ *and* $g \in C^1(\mathbb{R}^{K+1}, \mathbb{R})$*.*

Remark 6.3 *To realize more general kernels, we introduce the advection terms. Any continuous kernel J can be split into even one* J^e *and odd one* J^o*, i.e.,*

$$J^e(x) := \frac{J(x) + J(-x)}{2}, \quad J^o(x) := \frac{J(x) - J(-x)}{2}, \quad J(x) = J^e(x) + J^o(x).$$

By Corollary 6.1, for any $\varepsilon > 0$*, there are constants* d_j*,* α_j *(*$j = 0, \cdots, M$*) such that the even part* J^e *is approximated by* $\sum_{j=0}^{M} \alpha_j k^{d_j}$*.*

Next consider the approximation of the odd part. Set

$$G(x) := \int_0^x J^o(s) ds.$$

Since $\int_{\mathbb{T}} J^o(x) dx = 0$*, G is periodic in* $[-L, L]$*. By the integration by parts, we have* $J^o * u = G * u_x$*. As G is an even kernel, for any* $\varepsilon > 0$*, there are constants* d_j *and* α_j $(j = M+1, \cdots, K)$ *such that*

$$\Big\| \sum_{j=M+1}^{K} \alpha_j k^{d_j} - G \Big\|_{C_{per}(\mathbb{T})} \leq 2\varepsilon.$$

Thus, we can obtain

$$\Big\| J * u - \sum_{j=0}^{M} \alpha_j k^{d_j} * u - \sum_{j=M+1}^{K} \alpha_j k^{d_j} * u_x \Big\|_{C_{per}(\mathbb{T})} \leq 4\varepsilon \|u\|_{W^{1,1}(\mathbb{T})}$$

for any $u \in H^1(\mathbb{T})$*. By the above arguments, for any continuous kernel J, there are constants* d_j *and* α_j $(j = 0, \cdots, K)$ *such that*

$$\begin{cases} u_t &= d_u u_{xx} + g(u, \sum_{j=0}^{K} \alpha_j v_j), \\ 0 &= d_j v_{j,xx} + u - v_j, \quad (j = 0, \cdots, M) \\ 0 &= d_j v_{j,xx} + u_x - v_j, \quad (j = M+1, \cdots, K) \end{cases}$$

approximate (P)*. To approximate any continuous kernel, advection-reaction-diffusion systems are demanded.*

7 Numerical simulations

In the previous section, we have shown that any even functions can be realized by the reaction-diffusion system. In this section, we will investigate the profiles of stationary solutions of (7) in $\mathbb{T}$ numerically as the shape of the kernel varies. For the numerics, we utilize the simplified Mexican-hat kernel $J(x) = J(x;x_1)$ defined by

$$J(x;x_1) := e^{-c|x|} - m(x_1)e^{-c||x|-x_1|},$$

where c, x_1 are positive constants and $m(x_1)$ is a constant given by

$$m(x_1) := \frac{1-e^{-cL}}{2-e^{-c(L-x_1)}-e^{-cx_1}},$$

which implies the assumption ($A6$) of $J(x;x_1)$. Here x_1 corresponds to the position of the peak of the inhibitory region. The numerics are performed with $g(u,v) = uv + a(u-u^2)$ and the parameters as Fig. 1 (a) until $t = 100$. When numerical solutions satisfy $\sup_{t\in[90,100]} \|u(\cdot,t+\Delta t) - u(\cdot,t)\|_{C_{per}(\mathbb{T})} < 10^{-9}$, where $\Delta t = 10^{-2}$, we regard them as the "*stable stationary*" solutions for the initial data. We vary the value of x_1 and draw the profile of the stationary solution at $t = 100$.

As in Fig. 3, the inhomogeneous solutions with peaks are generated. The intervals and widths of the peaks of each stationary solution are equal. The number of the peaks in the stationary solution depends on the value of x_1. More precisely, the numbers of peaks in the results with $x_1 = 3, 5, 10, 15$ are $6, 4, 2$ and 1, respectively. Interestingly, when $x_1 = 13$, we obtain two stable stationary solutions depending on the initial data: one has one peak and the other has two peaks of which the widths are different as in Fig. 4 (a) and (b). Because all parameters of Fig. 4 (a) and (b) are same, these numerics suggest the existence of the secondary bifurcation. The Fourier coefficients of $J(x;x_1)$ can be calculated as follows:

$$\begin{aligned}&(\widehat{J}(\cdot;x_1))_k \\ &= \frac{2c}{c^2+(k\pi/L)^2}\left\{1-(-1)^k e^{-cL} + m(x_1)\left(e^{-cx_1} - 2\cos\frac{k\pi x_1}{L} + (-1)^k e^{-cL-cx_1}\right)\right\}.\end{aligned}$$

Accordingly, the eigenvalue (11) of the linearized problem of (7) with $x_1 = 13$ is shown in Fig. 5. We observe that the wave numbers from the primary eigenvalue to the forth one are $k = 2, 1, 5, 4$, respectively. From the widths of peaks of solutions in Fig. 4 (a) and (b), the solution in Fig. 4 (a) seems to correspond to $k = 2$, while that of (b) does to $k = 2$ and $k = 5$.

8 Concluding remarks

Firstly, we introduced a non-local evolution equation (P), in which a non-local interaction is imposed as the growth rate of the concentration as well as the dispersal term for the positive kernels by associating certain assumptions with g. We showed the global existence of solutions of (P) and the bifurcation from the homogeneous stable steady state. Accordingly, we determined that the homogeneous stable steady state may become unstable by adding non-local interaction, which we refer to as *non-local interaction induced instability*.

Subsequently, we proposed a reaction-diffusion system (RD^{ε}), with multiple components, which approximates the non-local evolution equation (P). Indeed, we showed that the solution of (RD^{ε}) converges to that of (P) as ε tends to 0 by the energy estimates. Through this approximation, we can regard the non-local interaction induced instability as diffusion-driven instability for the corresponding reaction-diffusion system (RD^{ε}). It has already been pointed out [7, 16, 17] that the Fourier transform of Mexican-hat type functions are peaked away from the origin and are capable of supporting the Turing instability by using a model such as (1). Our analysis supports their results from the difference perspective of the reaction-diffusion approximation.

The study of the eigenvalue problem (12) near the equilibrium point $(1, \mu, \mu)$ also implies that the stability depends on the parameters d_1 and d_2 determining the kernel shape. Additionally, the higher Fourier modes are stabilized by the diffusion term. Therefore, the balance between the diffusion effect and the non-local interaction plays a significant role to determine the patterns.

Moreover, we proved that any even convolution kernel can be approximated by the reaction-diffusion system. By controlling the coefficients of linear combinations among multiple components, specific symmetric global interactions can be created. Our analysis suggests that non-local interactions can be introduced as a result of the diffusion and reactions of multiple components.

In Section 7, we presented our investigation of the relationship of the profile of a kernel and the stationary solution. However, our understanding of this relationship is far from comprehensive and we plan to intensify our investigation thereof in future.

Acknowledgements

The authors would like to thank Professor Shin-Ichiro Ei of Hokkaido University for his fruitful suggestion for Remark 6.3 and to thank Professor Shintaro Kondo of Gifu University for his valuable comments. The first author is partially supported by JSPS KAKENHI Grant Numbers 26287024, 15K04963, 16K13778, 16KT0022. The second author has been supported by CREST, JST.

References

[1] S. Amari, *Dynamics of Pattern Formation in Lateral-Inhibition Type Neural Fields*, Biol. Cybernetics, **27**, (1977) 77-87

[2] A. Anma, K. Sakamoto, T. Yoneda, *Unstable subsystems cause Turing instability*, Kodai Math. J., **35**, (2012) 215-247

[3] P. W. Bates, P. C. Fife, X. Ren, X. Wang, *Traveling Waves in a Convolution Model for Phase Transitions*, Arch. Rational Mech. Anal. **138**, (1997) 105-136

[4] P. W. Bates, A. Chmaj, *An Integrodifferential Model for Phase Transitions: Stationary Solutions in Higher Space Dimensions*, Journal of Statistical Physics, **95**, (1999) 1119-1139

[5] P. W. Bates, G. Zhao, *Existence, uniqueness and stability of the stationary solution to a nonlocal evolution equation arising in population dispersal*, J. Math. Anal. Appl. **332**, (2007) 428-440

[6] H. Berestycki, G. Nadin, B. Perthame, L. Ryzhik, *The non-local Fisher-KPP equation: traveling waves and steady states*, Nonlinearity, **22**, (2009) 2813-2844

[7] S. Coombes, *Waves, bumps, and patterns in neural field theories*, Biological cybernetics, **93**, (2005) 91-108

[8] P. Fife, *Some nonclassical trends in parabolic and parabolic-like evolutions*, Trends in nonlinear analysis. Springer Berlin Heidelberg, (2003) 153-191

[9] J. Furter, M. Grinfeld, *Local vs. non-local interactions in population dynamics*, J. Math. Biol. **27**, (1989) 65-80

[10] D. Henry, *Geometric theory of semilinear parabolic equations*, Lecture Notes in Mathematics, 840. Springer-Verlag, Berlin-New York (1981)

[11] V. Hutson, S. Martinez, K. Mischaikow, G.T. Vickers, *The evolution of dispersal*, J. Math. Biol. **47**, (2003) 483-517

[12] S. Kondo, *An updated kernel-based Turing model for studying the mechanisms of biological pattern formation*, J. Theor. Biol. **414**, (2017) 120-127

[13] C. R. Laing, W. C. Troy, *Two-bump solutions of Amari-type models of neuronal pattern formation*, Physica D, **178**, (2003) 190-218

[14] C. R. Laing, W. Troy, *PDE methods for nonlocal models*, SIAM J. APPLIED DYNAMICAL SYSTEMS, **2**, (2003) 487-516

[15] R. Lefever, O. Lejeune, *On the origin of tiger bush*, Bull. Math. Biol. **59**, (1997) 263-294

[16] J. D. Murray, *Mathematical Biology. I. An introduction*, vol. **17** of Interdisciplinary Applied Mathematics. Springer, 3rd ed., (2002)

[17] J. D. Murray, *Mathematical Biology. II. Spatial models and biomedical applications*, vol. **18** of Interdisciplinary Applied Mathematics. Springer, 3rd ed., (2003)

[18] A. Nakamasu, G. Takahashi, A. Kanbe, S. Kondo, *Interactions between zebrafish pigment cells responsible for the generation of Turing patterns*, Proc. Natl. Acad. Sci. USA, **106**, (2009) 8429-8434

[19] R. Temam, *Infinite Dimensional Dynamical Systems in Mechanics and Physics*, vol. **68** of Applied Mathematical Sciences. Springer, 2nd ed., (1997)

[20] A.M. Turing, *The chemical basis of morphogenesis*. Phil. Trans. R. Soc. Lond. B, **237**, (1952) 37-72

[21] H. Yagisita, *Existence and Nonexistence of Traveling Waves for a Nonlocal Monostable Equation*, Publ. RIMS, Kyoto Univ., **45**, (2009) 925-953

A Appendix

A.1 Kernel

In this subsection, we consider the Green kernel of

$$-d_1 v'' + v = u \tag{19}$$

with periodic boundary condition. By using the variation of parameters from $x = -L$, we have the solution,

$$v_{-L}(x) = \frac{1}{2\sqrt{d_1}\sinh\frac{L}{\sqrt{d_1}}}\int_{-L}^{L}\cosh\left(\frac{y-x-L}{\sqrt{d_1}}\right)u(y)dy + \frac{1}{\sqrt{d_1}}\int_{-L}^{L}\chi_{y\le x}\sinh\left(\frac{y-x}{\sqrt{d_1}}\right)u(y)dy,$$

where $\chi_{y\le x}(y)$ is the characteristic function defined by

$$\chi_{y\le x}(y) := \begin{cases} 1 & (y \le x), \\ 0 & (y \ge x). \end{cases}$$

Similarly, we obtain the solution by using variation of parameters from $x = L$,

$$v_{L}(x) = \frac{1}{2\sqrt{d_1}\sinh\frac{L}{\sqrt{d_1}}}\int_{-L}^{L}\cosh\left(\frac{y-x+L}{\sqrt{d_1}}\right)u(y)dy + \frac{1}{\sqrt{d_1}}\int_{-L}^{L}\chi_{y\ge x}\sinh\left(\frac{y-x}{\sqrt{d_1}}\right)u(y)dy.$$

Due to the linearity of (19), $(v_{-L}(x)+v_L(x))/2$ is also a solution of (19). We denote it by $v_0(x)$. Before computing this, we recall two equalities:

$$\cosh A + \cosh B = 2\cosh\left((A+B)/2\right)\cosh\left((A-B)/2\right), \quad \cosh(A+B) = \cosh A\cosh B + \sinh A \sinh B$$

Usng $\chi_{y\le x} + \chi_{y\ge x} = (x-y)\,/\,|x-y|$ together with above equalities, we can compute that

$$\begin{aligned} v(x) &= \frac{1}{4\sqrt{d_1}\sinh\frac{L}{\sqrt{d_1}}}\int_{-L}^{L}\left(\cosh\left(\frac{y-x-L}{\sqrt{d_1}}\right)+\cosh\left(\frac{y-x+L}{\sqrt{d_1}}\right)\right)u(y)dy \\ &\quad + \frac{1}{2\sqrt{d_1}}\int_{-L}^{L}(\chi_{y\le x}+\chi_{y\ge x})\sinh\left(\frac{y-x}{\sqrt{d_1}}\right)u(y)dy \\ &= \frac{1}{2\sqrt{d_1}\sinh\frac{L}{\sqrt{d_1}}}\int_{-L}^{L}\cosh\left(\frac{L-|x-y|}{\sqrt{d_1}}\right)u(y)dy. \end{aligned}$$

The boundary condition is easily verified. By the definition (14) of k^d, $v = k^{d_1} * u$.

A.2 Proof of Theorem 3.2

We recall the uniform Gronwall lemma:

Lemma A.1 *(The uniform Gronwall Lemma [19, Lemma 1.1]) Let g, h, y be three positive locally integrable functions on $(t_0, +\infty)$ such that y' is locally integrable on $(t_0, +\infty)$, and which satisfy*

$$\frac{dy}{dt} \leq gy + h \quad for \quad t \geq t_0.$$

and

$$\int_t^{t+r} g(s)ds \leq a_1, \quad \int_t^{t+r} h(s)ds \leq a_2, \quad \int_t^{t+r} y(s)ds \leq a_3,$$

where r, a_1, a_2, a_3 are positive constants. Then

$$y(t+r) \leq \left(\frac{a_3}{r} + a_2\right)\exp(a_1), \quad {}^\forall t \geq t_0.$$

Proof of Theorem 3.2. Multiplying (P) by u and integrating over $\mathbb{T}$, we have

$$\frac{1}{2}\frac{d}{dt}\|u\|^2_{L^2(\mathbb{T})} = -d_u\|u_x\|^2_{L^2(\mathbb{T})} + \int_{\mathbb{T}} g(u, J*u)udx.$$

From the Cauchy-Schwarz inequality, the Young inequality for convolutions and the Hölder inequality, we have

$$\begin{aligned}
\int_{\mathbb{T}} g(u, J*u)udx &\leq -g_0\|u\|^{p+1}_{L^{p+1}(\mathbb{T})} + g_1\|J*u\|_{L^3(\mathbb{T})}\|u\|^2_{L^3(\mathbb{T})} + g_2\|J*u\|_{L^2(\mathbb{T})}\|u\|_{L^2(\mathbb{T})} + g_3\|u\|_{L^1(\mathbb{T})} \\
&\leq -g_0\|u\|^{p+1}_{L^{p+1}(\mathbb{T})} + g_1\|J\|_{L^1(\mathbb{T})}\|u\|^3_{L^3(\mathbb{T})} + g_2\|J\|_{L^1(\mathbb{T})}\|u\|^2_{L^2(\mathbb{T})} + g_3(2L)^{p/(p+1)}\|u\|_{L^{p+1}} \\
&\leq -g_0\|u\|^{p+1}_{L^{p+1}(\mathbb{T})} + g_1\|J\|_{L^1(\mathbb{T})}(2L)^{(p-2)/(p+1)}\|u\|^3_{L^{p+1}(\mathbb{T})} \\
&\quad + g_2\|J\|_{L^1(\mathbb{T})}(2L)^{(p-1)/(p+1)}\|u\|^2_{L^{p+1}(\mathbb{T})} + g_3(2L)^{p/(p+1)}\|u\|_{L^{p+1}(\mathbb{T})}.
\end{aligned}$$

Since $p \geq 3$, the Young inequality implies

$$\int_{\mathbb{T}} g(u, J*u)udx \leq -\frac{g_0}{4}\|u\|^{p+1}_{L^{p+1}(\mathbb{T})} + C_6,$$

where C_6 is a positive constant depending on $g_0, \cdots, g_3$, p, L and $\|J\|_{L^1(\mathbb{T})}$. By this estimate, we see that

$$\frac{1}{2}\frac{d}{dt}\|u\|^2_{L^2(\mathbb{T})} \leq -d_u\|u_x\|^2_{L^2(\mathbb{T})} - \frac{g_0}{4}\|u\|^{p+1}_{L^{p+1}(\mathbb{T})} + C_6.$$

Since $\|u(\cdot,t)\|_{L^2(\mathbb{T})}^{p+1} \le (2L)^{(p-1)/2}\|u(\cdot,t)\|_{L^{p+1}(\mathbb{T})}^{p+1}$ by the Hölder inequality, we obtain

$$\frac{1}{2}\frac{d}{dt}\|u\|_{L^2(\mathbb{T})}^2 \le -d_u\|u_x\|_{L^2(\mathbb{T})}^2 - \frac{g_0}{4}(2L)^{-(p-1)/2}\|u\|_{L^2(\mathbb{T})}^{p+1} + C_6.$$

Thus we get

$$\|u(\cdot,t)\|_{L^2(\mathbb{T})} \le C_7$$

for any $t \ge 0$, where

$$C_7 := \max\left\{\|u(\cdot,0)\|_{L^2(\mathbb{T})}, \left(\frac{4C_6(2L)^{(p-1)/2}}{g_0}\right)^{1/(p+1)}\right\}.$$

Therefore, u is bounded in $L^2(\mathbb{T})$ as long as the solution exists. Moreover integrating over $(t,t+r)$, we get

$$\int_t^{t+r}\|u_x(\cdot,s)\|_{L^2(\mathbb{T})}^2 ds \le \frac{C_6 r}{d_u} \tag{20}$$

for any positive t and r.

Next, differentiating (P) with respect to x, multiplying (P) by u_x and integrating over $\mathbb{T}$, we get

$$\begin{aligned}
\frac{1}{2}\frac{d}{dt}\|u_x\|_{L^2(\mathbb{T})}^2 &= -d_u\|u_{xx}\|_{L^2(\mathbb{T})}^2 + \int_{\mathbb{T}} g_u(u,J*u)u_x^2 dx + \int_{\mathbb{T}} g_v(u,J*u)u_x J*u_x dx \\
&\le -d_u\|u_{xx}\|_{L^2(\mathbb{T})}^2 - g_0 p\int_{\mathbb{T}}|u|^{p-1}u_x^2 dx + \int_{\mathbb{T}}(g_4|J*u|+g_5)u_x^2 dx \\
&\quad + \int_{\mathbb{T}}(g_6|u|+g_7)|u_x|\cdot|J*u_x|dx.
\end{aligned}\tag{21}$$

By $p \ge 3$, the Hölder inequality and the Young inequality we see that

$$\begin{aligned}
&\int_{\mathbb{T}}(g_6|u|+g_7)|u_x|\cdot|J*u_x|dx \\
\le\ & g_6\|J\|_{L^1(\mathbb{T})}\|u_x\|_{L^2(\mathbb{T})}\|u_x\|_{L^2(\mathbb{T})}^{(p-3)/(p-1)}\left(\int_{\mathbb{T}}|u|^{p-1}u_x^2\,dx\right)^{1/(p-1)} + g_7\|J\|_{L^1(\mathbb{T})}\|u_x\|_{L^2(\mathbb{T})}^2 \\
\le\ & g_0 p\int_{\mathbb{T}}|u|^{p-1}u_x^2\,dx + \frac{\|J\|_{L^1(\mathbb{T})}^{(p-1)/(p-2)}\|u_x\|_{L^2(\mathbb{T})}^2}{\{p(p-1)g_0\}^{1/(p-2)}} + g_7\|J\|_{L^1(\mathbb{T})}\|u_x\|_{L^2(\mathbb{T})}^2 \\
\le\ & g_0 p\int_{\mathbb{T}}u^{p-1}|u_x|^2 dx + C_8\|u_x\|_{L^2(\mathbb{T})}^2
\end{aligned}\tag{22}$$

with some positive constant C_8 independent of u. When $2 \leq p < 3$, (22) holds true by $g_6 = 0$. The Gagliardo-Nirenberg inequality implies

$$\int_{\mathbb{T}} g_4 |J*u||u_x|^2 dx \leq g_4 \|J\|_{L^1(\mathbb{T})} \|u\|_{L^2(\mathbb{T})} \|u_x\|^2_{L^4(\mathbb{T})} \leq \frac{d_u}{2} \|u_{xx}\|^2_{L^2(\mathbb{T})} + C_9 \|u_x\|^2_{L^2(\mathbb{T})},$$

where C_9 is a positive constant independent of u. Thus, applying the above inequality and (22) to (21), we obtain

$$\frac{1}{2}\frac{d}{dt}\|u_x\|^2_{L^2(\mathbb{T})} \leq -\frac{d_u}{2}\|u_{xx}\|^2_{L^2(\mathbb{T})} + (C_8 + C_9 + g_5)\|u_x\|^2_{L^2(\mathbb{T})}.$$

For $0 \leq t \leq r$,

$$\|u_x(\cdot,t)\|^2_{L^2(\mathbb{T})} \leq \|u_x(\cdot,0)\|^2_{L^2(\mathbb{T})} e^{2(C_8+C_9+g_5)r}.$$

Using (20) and applying Lemma A.1, we have shown the boundedness of $\|u_x(\cdot,t)\|^2_{L^2(\mathbb{T})}$ for any $t \geq r$. □

B Convergence

B.1 Proof of Theorem 5.1

In this section, we show the convergence of a solution of (RD^ε) to that of (P) under the assumptions $(A1)$–$(A5)$, where $J = J(x)$ is a linear combination of k^{d_j}. Let $u^0(x,t)$ be a solution of (P) with the initial datum $u(\cdot,0) = u_0(\cdot)$. Similarly, let $(u^\varepsilon, v_0^\varepsilon, \cdots, v_M^\varepsilon)$ be a solution of (RD^ε) with the initial datum $(u, v_0, \cdots, v_M)(\cdot,0) = (u_0, k^{d_0} * u_0, \cdots, k^{d_M} * u_0)(\cdot)$. To prove Theorem 5.1, we prepare the global bounds of solutions of (RD^ε).

Lemma B.1 *Assume that $u_0(x)$ belongs to $H^1(\mathbb{T})$. Then there exists a positive constant R_1 depending on $\|u_0(\cdot)\|_{H^1(\mathbb{T})}$ such that*

$$\|u^\varepsilon(\cdot,t)\|^2_{H^1(\mathbb{T})} \leq R_1, \quad \|v_j^\varepsilon(\cdot,t)\|^2_{H^1(\mathbb{T})} \leq R_1 \qquad (j = 0, \cdots, M) \tag{23}$$

for any $t \geq 0$ as long as the solution exists.

Proof of Lemma B.1. We only consider the case where $p \geq 3$ because we can treat the case where $2 \leq p < 3$ similarly. First show the L^2 boundedness. Multiplying the first equation of (RD^ε) by u^ε and using the argument similar to the proof of Theorem 3.2, we have

$$\frac{1}{2}\frac{d}{dt}\|u^\varepsilon\|_{L^2(\mathbb{T})}^2 \le -d_u\|u_x^\varepsilon\|_{L^2(\mathbb{T})}^2 - \frac{g_0}{4(2L)^{(p-1)/2}}\|u^\varepsilon\|_{L^2(\mathbb{T})}^{p+1} + C_{10}\sum_{j=0}^{M}\alpha_j^2\|v_j^\varepsilon\|_{L^2(\mathbb{T})}^2 + C_{11}, \tag{24}$$

where C_{10} and C_{11} are positive constants independent of ε and $(u^\varepsilon, v_0^\varepsilon, \cdots, v_M^\varepsilon)$. To estimate the $\|v_j^\varepsilon(\cdot,t)\|_{L^2(\mathbb{T})}^2$ $(j = 0, \cdots, M)$, multiplying the second equation of (RD^ε) by v_j^ε and integrating over $\mathbb{T}$, we have

$$\frac{1}{2}\frac{d}{dt}\|v_j^\varepsilon\|_{L^2(\mathbb{T})}^2 \le \frac{1}{\varepsilon}\left(-d_j\|v_{j,x}^\varepsilon\|_{L^2(\mathbb{T})}^2 - \frac{1}{2}\|v_j^\varepsilon\|_{L^2(\mathbb{T})}^2 + \frac{1}{2}\|u^\varepsilon\|_{L^2(\mathbb{T})}^2\right). \tag{25}$$

Multiplying the above inequalities by α_j and adding them with respect to j, it follows that

$$\varepsilon\frac{d}{dt}\sum_{j=0}^{M}\alpha_j^2\|v_j^\varepsilon\|_{L^2(\mathbb{T})}^2 \le -2\sum_{j=0}^{M}\alpha_j^2 d_j\|v_{j,x}^\varepsilon\|_{L^2(\mathbb{T})}^2 - \sum_{j=0}^{M}\alpha_j^2\|v_j^\varepsilon\|_{L^2(\mathbb{T})}^2 + \left(\sum_{j=0}^{M}\alpha_j^2\right)\|u^\varepsilon\|_{L^2(\mathbb{T})}^2 \tag{26}$$

Setting

$$X(t) := \|u^\varepsilon(\cdot,t)\|_{L^2(\mathbb{T})}^2, \quad Y(t) := \sum_{j=0}^{M}\alpha_j^2\|v_j^\varepsilon(\cdot,t)\|_{L^2(\mathbb{T})}^2,$$

we see that the region

$$\left\{(X,Y)\in\mathbb{R}^2 \mid 0 \le X \le R, \quad 0 \le Y \le 2R\sum_{j=0}^{M}\alpha_j^2\right\}$$

is positively invariant, where R is a positive constant satisfying

$$R \ge \|u_0\|_{L^2(\mathbb{T})}^2, \quad \frac{g_0}{4(2L)^{(p-1)/2}}R^{(p+1)/2} > C_{10}\max\left\{2R\sum_{j=0}^{M}\alpha_j^2, \sum_{j=0}^{M}\alpha_j^2\|k^{d_j} * u_0\|_{L^2(\mathbb{T})}^2\right\} + C_{11}$$

Then, applying the theory of the positively invariant region to (24) and (26), we have

$$\|u^\varepsilon(\cdot,t)\|_{L^2(\mathbb{T})}^2 \le R, \quad \sum_{j=0}^{M}\alpha_j^2\|v_j^\varepsilon(\cdot,t)\|_{L^2(\mathbb{T})}^2 \le 2R\sum_{j=0}^{M}\alpha_j^2.$$

Thus we have shown that

$$\|u^{\varepsilon}(\cdot,t)\|_{L^2(\mathbb{T})}^2 \le R_0, \quad \sum_{j=0}^{M} \alpha_j^2 \|v_j^{\varepsilon}(\cdot,t)\|_{L^2(\mathbb{T})}^2 \le R_0$$

for any $t \ge 0$ as long as the solution exists, by taking $R_0 := R \cdot \max\{1, 2\sum_{j=0}^{M} \alpha_j^2\}$.

Next we consider the estimate of u_x^{ε} and $v_{j,x}^{\varepsilon}$. Integrating (24) and (25) over $[t, t+r]$ yields

$$\begin{cases} \displaystyle\int_t^{t+r} \|u_x^{\varepsilon}(\cdot,s)\|_{L^2(\mathbb{T})}^2 ds \;\le\; (C_{10}R_0 + C_{11})\frac{r}{d_u} + \frac{R_0}{d_u}, \\ \displaystyle\int_t^{t+r} \|v_{j,x}^{\varepsilon}(\cdot,s)\|_{L^2(\mathbb{T})}^2 ds \;\le\; \frac{R_0 r}{2d_j} + \frac{R_0}{d_j \alpha_j^2}, \qquad (j = 0, \cdots, M) \end{cases} \tag{27}$$

for any $t \ge 0$, $r > 0$ and $0 < \varepsilon \le 1$. Differentiating the first equation of (RD^{ε}) with respect to x and applying the argument similar to the proof of Theorem 3.2 yield

$$\frac{1}{2}\frac{d}{dt}\|u_x^{\varepsilon}\|_{L^2(\mathbb{T})}^2 \le -\frac{d_u}{2}\|u_{xx}^{\varepsilon}\|_{L^2(\mathbb{T})}^2 + C_{12}\|u_x^{\varepsilon}\|_{L^2(\mathbb{T})}^2 + C_{12}\sum_{j=0}^{M}\alpha_j^2\|v_j^{\varepsilon}\|_{L^2(\mathbb{T})}^2, \tag{28}$$

where C_{12} is a positive constant independent of ε and $(u^{\varepsilon}, v_0^{\varepsilon}, \cdots, v_M^{\varepsilon})$. By the equation for v_j in (RD^{ε}), we get

$$\varepsilon\frac{d}{dt}\|v_{j,x}^{\varepsilon}\|_{L^2(\mathbb{T})}^2 \le -2d_j\|v_{j,xx}^{\varepsilon}\|_{L^2(\mathbb{T})}^2 - \|v_{j,x}^{\varepsilon}\|_{L^2(\mathbb{T})}^2 + \|u_x^{\varepsilon}\|_{L^2(\mathbb{T})}^2, \tag{29}$$

It follows from (28) and (29) that $\|u_x^{\varepsilon}\|_{L^2(\mathbb{T})}^2$ and $\|v_{j,x}^{\varepsilon}\|_{L^2(\mathbb{T})}^2$ is bounded for $0 \le t \le r$ with any $r > 0$. Applying Lemma A.1 to (28) and (29) with (27), we can obtain the boundedness of $\|u_x(\cdot,t)\|_{L^2(\mathbb{T})}$ and $\|v_{j,x}(\cdot,t)\|_{L^2(\mathbb{T})}$ for any $t \ge r$. Hence we have obtained (23). □

Proof of Theorem 5.1. This proof is also based on the energy method. We firstly estimate the convergence of $u^{\varepsilon} \to u^0$ in $L^2(\mathbb{T})$ as $\varepsilon \to 0$. Denoting the difference of the solution $u^{\varepsilon} - u^0$ by $U(x,t)$ and taking the difference between the first equation of (RD^{ε}) and (P), we have

$$U_t = d_u U_{xx} + g(u^{\varepsilon}, \sum_{j=0}^{M}\alpha_j v_j^{\varepsilon}) - g(u^0, J * u^0). \tag{30}$$

Set

$$V_j := v_j^\varepsilon - k^{d_j} * u^\varepsilon, \quad \rho_j := k^{d_j} * u^\varepsilon,$$

where k^d is defined by (14). By the argument in Appendix A.1, ρ_j satisfies

$$0 = d_j \Delta \rho_j - \rho_j + u^\varepsilon \qquad (j = 0, \cdots, M) \tag{31}$$

and

$$\sum_{j=0}^{M} \alpha_j \rho_j = J * u^\varepsilon.$$

Multiplying (30) by $U(x,t)$ and integrating over $\mathbb{T}$, we find from the mean value theorem that

$$\begin{aligned}
\frac{1}{2}\frac{d}{dt}\|U\|^2_{L^2(\mathbb{T})} &= -d_u\|U_x\|^2_{L^2(\mathbb{T})} + \int_{\mathbb{T}} g_u((1-\theta_1)u^0 + \theta_1 u^\varepsilon, \sum_{j=0}^{M}\alpha_j v_j^\varepsilon)U^2 dx \\
&\quad + \int_{\mathbb{T}} g_v(u^0, \sum_{j=0}^{M}\alpha_j((1-\theta_2)\rho_j + \theta_2 v_j^\varepsilon)) \sum_{j=0}^{M}\alpha_j V_j \cdot U dx \\
&\quad + \int_{\mathbb{T}} g_v(u^0, (1-\theta_3)J * u^0 + \theta_3 J * u^\varepsilon)(J * U)U dx
\end{aligned}$$

for some θ_1, θ_2, $\theta_3 \in (0,1)$ depending on x, u^0, u^ε and so on. By $(A3)$ and $(A4)$, we have

$$\begin{aligned}
\frac{1}{2}\frac{d}{dt}\|U\|^2_{L^2(\mathbb{T})} &\leq -d_u\|U_x\|^2_{L^2(\mathbb{T})} + \int_{\mathbb{T}} \Big(-g_0 p|(1-\theta_1)u^0 + \theta_1 u^\varepsilon|^{p-1} + g_4\Big|\sum_{j=0}^{M}\alpha_j v_j^\varepsilon\Big| + g_5\Big)U^2 dx \\
&\quad + (g_6\|u^0\|_{C(\mathbb{T})} + g_7)\int_{\mathbb{T}}\Big|\sum_{j=0}^{M}\alpha_j V_j U\Big| dx + (g_6\|u^0\|_{C(\mathbb{T})} + g_7)\|J\|_{L^1(\mathbb{T})}\|U\|^2_{L^2(\mathbb{T})}
\end{aligned} \tag{32}$$

as $u^0(\cdot,t) \in C_{per}(\mathbb{T})$ from Theorem 3.2 and the Sobolev embedding theorem. It follows from Lemma B.1 and

$$\rho_{j,t} = k^{d_j} * u_t^\varepsilon = k^{d_j} * \Big(d_u u_{xx}^\varepsilon + g(u^\varepsilon, \sum_{j=0}^{M}\alpha_j v_j^\varepsilon)\Big) = \frac{d_u}{d_j}\Big(k^{d_j} * u^\varepsilon - u^\varepsilon\Big) + k^{d_j} * \Big(g(u^\varepsilon, \sum_{j=0}^{M}\alpha_j v_j^\varepsilon)\Big)$$

through the integration by parts, that there is a positive constant R_2 independent of ε and $(u^\varepsilon, v_0^\varepsilon, \cdots, v_M^\varepsilon)$ satisfying

$$\|\rho_{j,t}\|_{H^1(\mathbb{T})} \leq R_2 \tag{33}$$

for any $t \geq 0$ and $j = 0, \cdots, M$.

Since $\varepsilon(V_{j,t} + \rho_{j,t}) = d_j V_{j,xx} - V_j$ by (31), we get

$$\begin{aligned} \varepsilon \int_{\mathbb{T}} V_{j,t} V_j dx &= -\varepsilon \int_{\mathbb{T}} \rho_{j,t} V_j dx - d_j \|V_{j,x}\|^2_{L^2(\mathbb{T})} - \|V_j\|^2_{L^2(\mathbb{T})} \\ &\leq \frac{\varepsilon^2}{2} \|\rho_{j,t}\|^2_{L^2(\mathbb{T})} - d_j \|V_{j,x}\|^2_{L^2(\mathbb{T})} - \frac{1}{2} \|V_j\|^2_{L^2(\mathbb{T})}, \end{aligned}$$

which implies

$$\frac{1}{2} \frac{d}{dt} \|V_j\|^2_{L^2(\mathbb{T})} \leq \frac{\varepsilon R_2^2}{2} - \frac{1}{2\varepsilon} \|V_j\|^2_{L^2(\mathbb{T})}$$

by (33). Thus we obtain

$$\|V_j\|_{L^2(\mathbb{T})} \leq \varepsilon R_2 \tag{34}$$

because $V_j(x,0) = v_j^\varepsilon(x,0) - (k^{d_j} * u_0)(x) \equiv 0$. Applying (34), Lemma B.1 and Theorem 3.2 to (32) yields

$$\frac{d}{dt} \|U\|^2_{L^2(\mathbb{T})} \quad \leq \quad C_{13} \|U\|^2_{L^2(\mathbb{T})} + C_{14} \varepsilon^2, \tag{35}$$

where C_{13}, C_{14} are positive constants. Thus, from the classical Gronwall inequality, we see that

$$\|U\|^2_{L^2(\mathbb{T})} \leq \frac{C_{14}}{C_{13}} (e^{C_{13} t} - 1) \varepsilon^2$$

because $U(x,0) = u^\varepsilon(x,0) - u^0(x,0) \equiv 0$. This inequality implies the convergence of u^ε to u^0 on any finite interval $[0,T]$.

Next we show that $\left\| u_x^\varepsilon - u_x^0 \right\|_{L^2(\mathbb{T})} \to 0$ as $\varepsilon \to 0$ in the similar manner. Multiplying (30) by $-U_{xx}$, integrating that over $\mathbb{T}$ and using the Schwarz inequality, we see that

$$\begin{aligned} \frac{1}{2} \frac{d}{dt} \|U_x\|^2_{L^2(\mathbb{T})} &\leq -\frac{d_u}{2} \|U_{xx}\|^2_{L^2(\mathbb{T})} + \frac{1}{2d_u} \left\| g(u^\varepsilon, \sum_{j=0}^{M} \alpha_j v_j^\varepsilon) - g(u^0, J * u^0) \right\|^2_{L^2(\mathbb{T})} \\ &\leq \frac{1}{2d_u} \left\| g(u^\varepsilon, \sum_{j=0}^{M} \alpha_j v_j^\varepsilon) - g(u^0, J * u^0) \right\|^2_{L^2(\mathbb{T})}. \end{aligned}$$

Using the mean value theorem and the boundedness of u^0, u^ε in $C_{per}(\mathbb{T})$, we have

$$\frac{1}{2} \frac{d}{dt} \|U_x\|^2_{L^2(\mathbb{T})} \quad \leq \quad \frac{C_{15}}{2} \left(\|U\|^2_{L^2(\mathbb{T})} + \sum_{j=0}^{M} \|V_j\|^2_{L^2(\mathbb{T})} \right).$$

Hence, by (34), we see that

$$\|U_x\|^2_{L^2(\mathbb{T})} \le C_{15}\left(\frac{C_{14}}{C_{13}}(e^{C_{13}t}-1)+MR_2^2\right)\varepsilon^2,$$

where C_{15} is a positive constant independent of ε and $(u^\varepsilon, v_0^\varepsilon, \cdots, v_M^\varepsilon)$. We have completed the proof of Theorem 5.1. □

B.2 Proof of Lemma 6.1

Proof of Lemma 6.1. From Theorem 3.2, $\sup_{0\le t\le T}\|u_j\|_{C_{per}(\mathbb{T})}$ $(j=1,2)$ are bounded. Setting $U=u_1-u_2$, we have

$$U_t = d_u U_{xx} + g(u_1, J_1 * u_1) - g(u_2, J_2 * u_2).$$

Multiplying U to the above equation and integrate over $\mathbb{T}$, we get

$$\frac{1}{2}\frac{d}{dt}\|U\|^2_{L^2(\mathbb{T})} \le -d_u\|U_x\|^2_{L^2(\mathbb{T})} + C_{16}\|U\|^2_{L^2(\mathbb{T})} + C_{16}\|J_1-J_2\|_{L^1(\mathbb{T})}\|U\|_{L^2(\mathbb{T})}$$

with some positive constant C_{16}. Similarly, we also obtain

$$\frac{1}{2}\frac{d}{dt}\|U_x\|^2_{L^2(\mathbb{T})} \le -\frac{d_u}{2}\|U_{xx}\|^2_{L^2(\mathbb{T})} + C_{17}\|U\|^2_{L^2(\mathbb{T})} + C_{17}\|J_1-J_2\|^2_{L^1(\mathbb{T})}.$$

Thus we can conclude this lemma. □

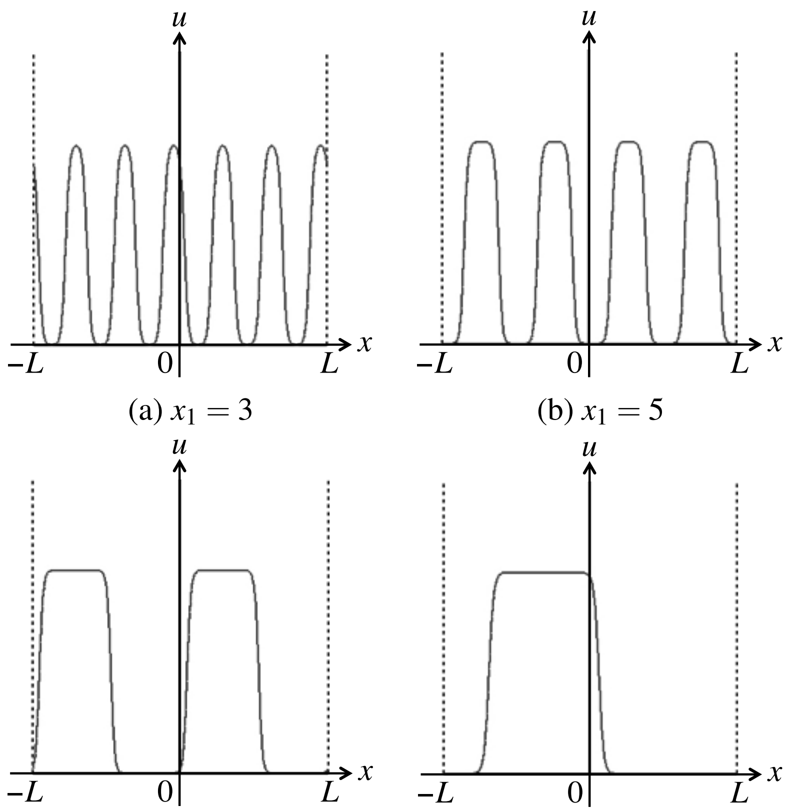

(a) $x_1 = 3$ (b) $x_1 = 5$

(c) $x_1 = 10$ (d) $x_1 = 15$

Figure 3: Numerical results of the model (7) at $t = 100$ with $J(x;x_1)$ and the same parameters as Fig. 1. The vertical axis is the value of u and the horizontal axis is the position x. The results with $x_1 = 3$, $x_1 = 5$, $x_1 = 10$ and $x_1 = 15$ correspond to (a), (b), (c) and (d), respectively.

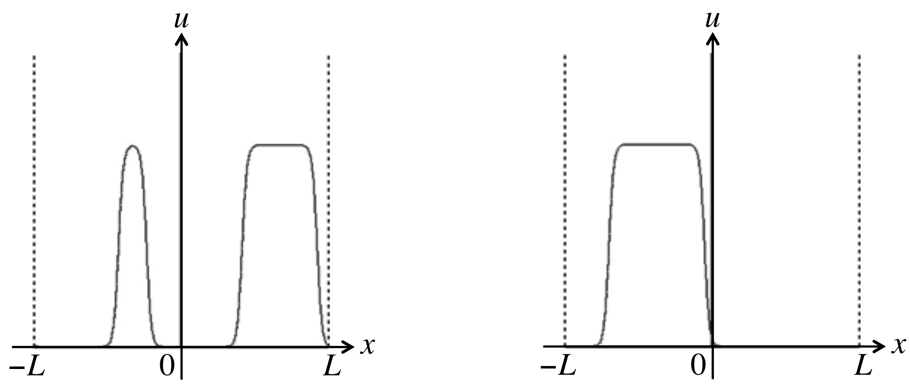

(a) Maximum eigenvalue for $x_1 = 13$ (b) Second largest eigenvalue for $x_1 = 13$

Figure 4: Numerics of the model (7) with $x_1 = 13$ and same parameters as Fig. 3. The different shapes of the solutions (a) and (b) caused by the different initial data.

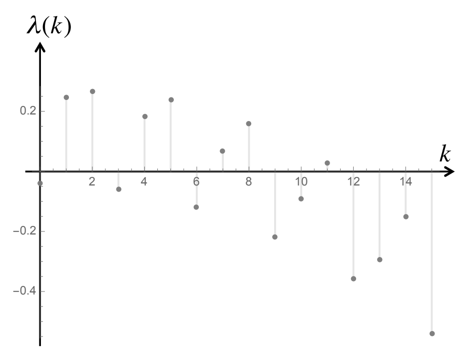

Figure 5: Relationship between the eigenvalues and wave number for $x_1 = 13$.